Age Classification using Facial Feature Extraction

Fatemeh Mirzaei

Submitted to the
Institute of Graduate Studies and Research
in partial fulfillment of the requirements for the Degree of

Master of Science
in
Computer Engineering

Eastern Mediterranean University
January 2011
Gazimağusa, North Cyprus

Approval of the Institute of Graduate Studies and Research

Prof. Dr. Elvan Yılmaz
Director (a)

I certify that this thesis satisfies the requirements as a thesis for the degree of Master of Science in Computer Engineering.

Assoc. Prof. Dr. Muhammed Salamah
Chair, Department of Computer Engineering

We certify that we have read this thesis and that in our opinion it is fully adequate in scope and quality as a thesis for the degree of Master of Science in Computer Engineering.

Asst. Prof. Dr. Önsen Toygar
Supervisor

Examining Committee

1. Assoc. Prof. Dr. Hasan Demirel _____
2. Asst. Prof. Dr. Önsen Toygar _____
3. Asst. Prof. Dr. Ahmet Ünveren _____

ABSTRACT

This thesis presents age classification on facial images using Local Binary Patterns (LBP) and modular Principal Component Analysis (mPCA) as subpattern-based approaches and holistic Principal Component Analysis (PCA) and holistic subspace Linear Discriminant Analysis (ssLDA) methods. Classification of age intervals are conducted separately on female and male facial images since the aging process for female and male is different for human beings in real life. The age classification performance of the holistic approaches is compared with the performance of subpattern-based LBP and mPCA approaches in order to demonstrate the performance differences between these two types of approaches. Our work has been tested on two aging databases namely FGNET and MORPH. The experiments are performed on these aging databases to demonstrate the age classification performance on female and male facial images of human beings using subpattern-based LBP method with several parameter settings. The results are then compared with the results of age classification using mPCA method, holistic PCA and subspace LDA methods.

Keywords – Age Classification, Local Binary Patterns, Modular Principal Component Analysis, Principal Component Analysis, Subspace Linear Discriminant Analysis.

ÖZ

Bu tezde alt-örüntüye dayalı Yerel İkili Örüntü (LBP) ve modüler Ana Bileşenler Analizi (mPCA) yaklaşımlarının yanısıra bütünsel Ana Bileşenler Analizi (PCA) ve altuzay Doğrusal Ayırtaç Analizi (ssLDA) yöntemleri kullanılarak yüz resimlerinin yaş sınıflandırması sunulmuştur. Gerçek hayatta kadın ve erkeklerin yaşlanma süreci farklı olduğundan dolayı, yaş aralıklarının belirlenmesi kadın ve erkek resimleri üzerinde ayrı olarak incelenmiştir. Alt-örüntüye dayalı LBP ve mPCA yaklaşımlarının yaş sınıflandırma performansı, bütünsel yaklaşımlarla karşılaştırılmış ve bu iki çeşit yaklaşımın performans farklılıkları sunulmuştur. Bu çalışmadaki deneyler yaygın olarak kullanılan FGNET ve MORPH isimli yaşlanma veritabanları üzerinde yapılmıştır. Kadın ve erkek resimleri kullanılarak yapılan yaş sınıflandırmasının performansını göstermek için alt-örüntüye dayalı LBP yöntemi değişik parametre değerleri ile yaşlanma veritabanları kullanılarak çalıştırılmıştır. Bu deneylerin sonuçları daha sonra mPCA, bütünsel PCA ve altuzay LDA yöntemleri kullanılarak yapılan yaş sınıflandırması deney sonuçlarıyla karşılaştırılmıştır.

Anahtar Kelimeler: Yaş Sınıflandırması, Yerel İkili Örüntü, modüler Ana Bileşenler Analizi, Ana Bileşenler Analizi, Altuzay Doğrusal Ayırtaç Analizi.

DEDICATION

This is a dedication to the love of my life, My Husband, I would like to Thank You for 2 and half wonderful years, through all the ups and downs. You're Still The One.

I also dedicate this thesis to my BELOVED PARENTS, who are a part of my heart, and I will be grateful all the days of my life for having had the honor to be your daughter.

ACKNOWLEDGMENTS

The sincere thanks go to my advisor Asst. Prof. Dr. Önsen Toygar whose patience and encouragement guided me during the research. This dissertation would never be possible without her helps. To me, she is not only the perfect mentor but also a true friend. I also thank Assoc. Prof. Dr. Hasan Demirel and Asst. Prof. Dr. Ahmet Ünveren for serving on my thesis committee.

My warmest thank to my dear husband, Amin. Whenever I encounter the difficulties and disappointment, he always consoled me with the cordial warmth. He gave me confident to go on and never hesitates to patiently assist me through the master study. I am blessed to have him by my side and in my life.

I would like to express my heart-felt gratitude to my dear parents for their constant source of love, patients and encouragements through my life.

TABLE OF CONTENTS

LIST OF TABLES

LIST OF FIGURES

Chapter 1

INTRODUCTION

Face images convey a significant amount of information including information about the identity, emotional state, ethnic origin, gender, age, and head orientation of a person shown in a face image [1]. In this study the age interval of facial images is extracted for age classification purpose. Age classification has been studied in the literature either as classification of age intervals to estimate an age group or as age estimation to estimate an exact age. Some of the applications of age classification are listed below.

1.1 Motivation

There are lots of applications that can benefit from automated systems. Age determination can be used in a variety of applications ranging from access control, human machine interaction, person identification, data mining and organization. Examples can demonstrate some uses of the aging software for each category mentioned above.

1.1.1 Age-Based Access Control

Age-based restrictions apply to physical or virtual access in some real life applications. For example age-related entrance restrictions may apply to different premises, web pages or even for preventing the purchase of certain goods (e.g. alcoholic drinks or cigarettes) by under-aged individuals [3]. Secure Internet access control is another example in order to ensure that under-aged persons can not access to Internet pages with unsuitable material.

1.1.2 Age Specific Human Computer Interaction (ASHCI)

If computers could determine the age of the user, both the computing environment and the type of interaction could be adjusted according to the age of the user [1]. Automatically adjusting the user interface of the computer or machine users to suit the needs of users age group is one of the applications in ASHCI [31]. For example, text and icons of the interface can be changed according to the users age, if he or she is old the text with large font will be more suitable. On the other hand icons could be more activated for young users. So persons with different age groups have different requirements and needs related to the way they interact with computers or other machines.

1.1.3 Age Invariant Person Identification

Automatic age estimation systems could form the basis of designing automatic age progression systems. (i.e., systems with the ability to predict the future facial appearance of subjects). One of the most popular applications of age progression systems is “Missing Children” and it creates an image to investigate what a missing child would look like today [1].

1.1.4 Data Mining and Organization

Age-based retrieval and classification would enable the users to automatically sort and retrieve the images from e-photo albums and the Internet by specifying a required age-range [31].

1.2 Related Works

Age classification has been studied in the literature either as classification of age intervals to estimate an age group or as age estimation to estimate an exact age. Age classification and age estimation problems are solved similarly using classification

methods to produce an output for the test images either as an age interval or as an exact age. Kwon and Lobo [2] classified ages from facial images into 3 age groups as babies, young adults and senior adults. They used cranio facial development theory and skin wrinkle analysis in their study. Using the primary features of the human face such as eyes, nose, mouth, chin and virtual top of the head; mainly 6 different ratios are calculated to distinguish babies from young adults and senior adults. Then they used secondary feature analysis with a wrinkle geography map to detect and measure wrinkles to distinguish seniors from babies and young adults. Finally, they combined ratios and wrinkle information obtained from facial images to classify faces into 3 age groups.

Lanitis et.al in [1] mainly investigated 3 different classifiers for automatic age estimation. They compared a quadratic function based classifier, a shortest distance classifiers and neural network based classifiers. Supervised and unsupervised neural networks such as multilayer perceptrons (MLPs) and Kohonen Self Organizing Map (SOM) are investigated for age estimation experiments. The facial images used in the experiments range from 0 to 35 years and the ages are classified into 3 categories for the age ranges of 0-10 years, 11-20 years and 21 to 35 years.

Geng et.al [4] proposed a subspace approach named AGES (Aging pattErn Subspace) for automatic age estimation, modeling the aging patterns by a representative subspace. They categorize the facial images from FG-NET and MORPH databases into age ranges of 0-9, 10-19, 20-39 and 40-69. AGES algorithm models the aging pattern which is defined as a sequence of a particular individual's face images sorted in time order by constructing a representative subspace.

Yang and Ai [5] investigated demographic classification using age, gender and ethnicity information with Local Binary Pattern (LBP). They classified age into 3 categories as child, youth and oldness. Age classification is performed by first classifying children and then separating oldness age group from youth. The experiments using FERET, PIE and snapshot images classify gender (as female and male) age (as 3 age groups) and ethnicity (as Asian or non-Asian) effectively using LBP histogram (LBPH) features.

Fu and Huang [6] proposed a method for age estimation through quadratic regression on the discriminative aging manifolds. The experiments are performed separately on female and male facial images. They suggested that the correlation between group truth age is different for female and males, therefore the experiment are considered separately for male and female age estimation. A low dimensional aging manifold subspace is first found by using conformal embedding analysis and the manifold representation is modeled with a multiple linear regression procedure based on a quadratic function. The experiments are performed using several methods to estimate the exact age or an age interval for males and females separately.

Guo et al.[31] introduce the age manifold learning scheme for extracting face aging features and design a locally adjusted robust regressor for learning and prediction of human ages. They used an internal age database UIUC-IFP-Y and publicly available FG-NET database. Age estimation experiments are done on female and male images separately. Finally, Lanitis [32] summarized the effects of aging in his latest article for many different biometrics including face, iris, fingerprint, etc.

1.3 Overview

As humans, we are able to categorize human age groups from their face and facial images and are often able to be quite precise in this estimation but computers cannot detect it easily. Aging has a number of dramatic effects on the face. The physical/biological changes that occur on the face provide the physical cues for judgments of age [7]. Aging process can be determined by person's gene, external factors such as health, living style, living location, weather conditions. Males and females age differently because of the factors such as makeup and accessories mostly used by females. On the other hand, biological factors such as bone growth, loss in elasticity of facial muscles affect the aging. Additionally, other factors such as ethnicity, gender, dietary habits and climatic conditions have some effect on aging.

Shape and texture variations affect the aging process during different years. Textural variations in the form of wrinkles and other skin artifacts take precedence over shape variations during later stages of adulthood [8]. The geometric transformation is one of the shape variations that appear in human faces during formative years (0 to 18 years). Cardioidal strain transformation, affine shear transformation, revised-cardioidal strain transformation, spiral strain transformation are some of transformation functions that were studied in relevance to facial growth. Figure 1.1 illustrates the effects of these four transformation functions.

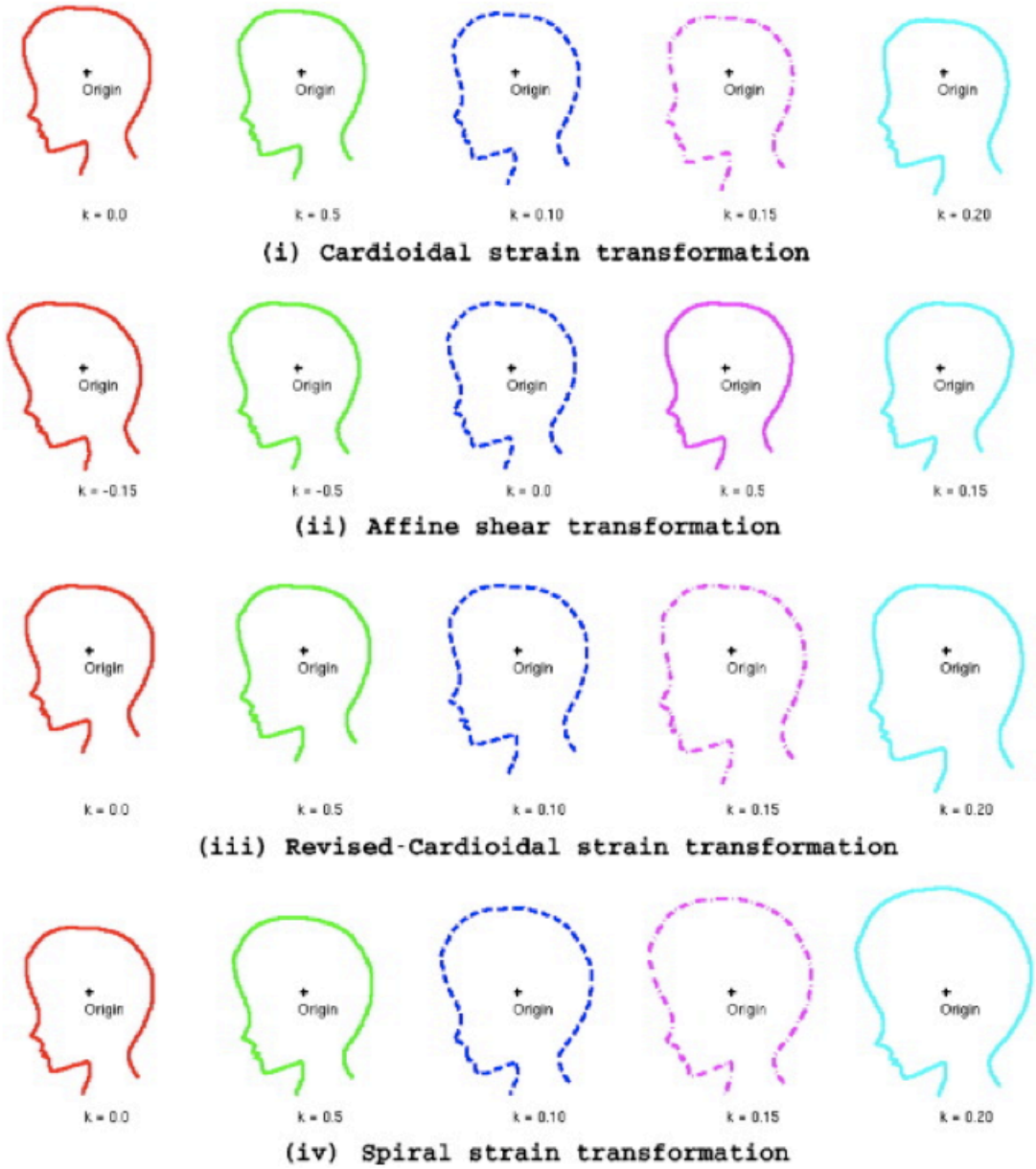

Figure 1.1: An illustration of the effects of applying different transformation functions on 'profile faces' [9].

1.3.1 Age Classification from Facial Images

Age estimation is the determination of person's age based on biometric features. Although age estimation can be accomplished using different biometric traits, this thesis is focused on facial age classification that relies on biometric features extracted from a person's face [3]. Age estimation will be more accurate when shape

and skin features are taken into consideration. The basis of this thesis is a statistical analysis of facial features in order to classify the facial images according to corresponding age intervals.

1.4 The Work Done In This Study

In this study supervised learning is used to train the computer with a specific number of training facial images. The relationship between the coded representation of the training faces' ages and the actual ages of the test subjects is then learnt. Once this relationship is established, it is possible to estimate the age of a previously unseen image. Regarding to this issue shape variation analysis is done by categorizing the differences between ratios during formative years, in order to classify the facial images, texture analysis is applied on female and male facial images separately by four different techniques namely LBP (Local Binary Pattern) and mPCA (modular Principal Component Analysis) as subpattern-based approaches, and, PCA (Principal Component Analysis) and ssLDA (subspace Linear Discriminant Analysis) as holistic methods (the process of applying one of the various algorithms to the whole-face) are used as feature extractors with the combination of the preprocessing techniques of histogram equalization (HE) and mean-and-variance normalization (MVN) in order to minimize the effect of illumination.

The success and popularity of these algorithms are mainly due to their statistics-based ability of automatically deriving the features instead of relying on humans for their definitions. These algorithms are widely studied for the recognition and classification of human beings. Although these feature extraction algorithms are successful, they are not perfect as there are many obstacles such as changes in illumination, pose, facial expression, facial texture (e.g. wrinkles), and shape (e.g.

weight gain or loss), facial hair, presence of partial occlusions (e.g. glasses, scarf) and age progression [10] as shown in Figures 1.2 through 1.8.

Figure 1.2: Difference in Illumination (a) Brighter image (b) Darker image

Figure 1.3: Difference in Pose (a) Frontal image (b) Profile image with some angle.

Figure 1.4: Difference in Facial Expression (a) Angry Face (b) Happy Face.

Figure 1.5: Difference in Facial Texture (a) Image without wrinkles (b) Image with wrinkles.

Figure 1.6: Difference in Facial Texture (a) Normal Face (b) Makeup Face

Figure 1.7: Difference in Facial Hair (a) Face without mustache and beard (b) Face with mustache and beard.

Figure 1.8: Presence of Partial Occlusions (a) Face without glasses (b) Face with glasses.

The holistic and subpattern-based approaches are implemented using the cropped face images from two different datasets selected from MORPH [30] and FG-NET [29] databases. Various experiments are performed to test the classification performance of the LBP, mPCA, original PCA, subspace LDA approaches. The results are presented in the further sections. The accuracy of age classification of

female and male are compared with the four methods mentioned above. Finally in order to decrease the age range interval, the second step of classification is done right after the first step of classification.

The rest of the thesis is organized as follows. Chapter 2 presents the preprocessing steps to prepare images for training and testing phases. In Chapter 3, the methods used for facial feature extraction are discussed. Chapter 4 presents the geometric variation on face images across age progression. The experimental results for age classification on female and male facial images are demonstrated in Chapter 5. Finally, Chapter 6 presents the conclusions.

Chapter 2

PREPROCCESSING

Images of subjects captured by camera will normally be out of phase with each other because of difference in background, pose of head, contrast of images, number of intensity levels, size of the images and other causes. Most of the programs cannot automatically solve all of these problems. Therefore some of the deficiencies of these images should be solved before defining them to the program as input and some of them should be solved during process of classification. Figure 2.1 shows the processes that took place to prepare images for being used in facial age classification algorithm.

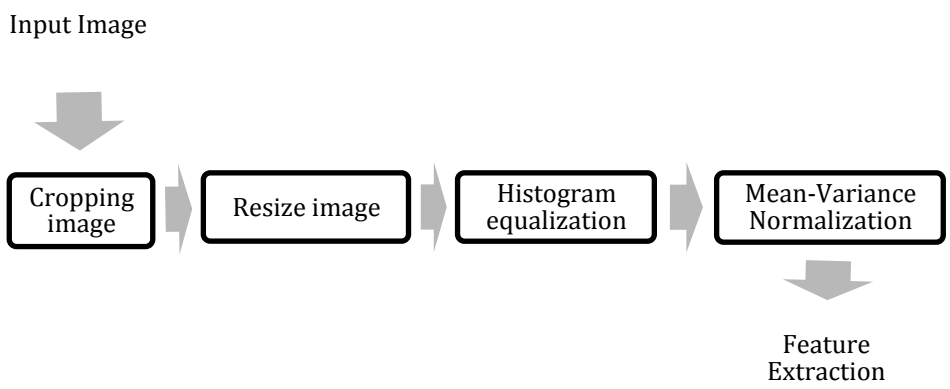

Figure 2.1: Preprocessing steps on images

2.1 Cropping Images

The background of the image and some part of face like hairs and neck are sources of failure in the classification of facial ages efficiently. Therefore they should be removed from the image. Figure 2.2 shows the difference between initial image and cropped image. The other reason of cropping is to decrease memory consumption and increase the speed of detecting age because vast useless data has removed from the image.

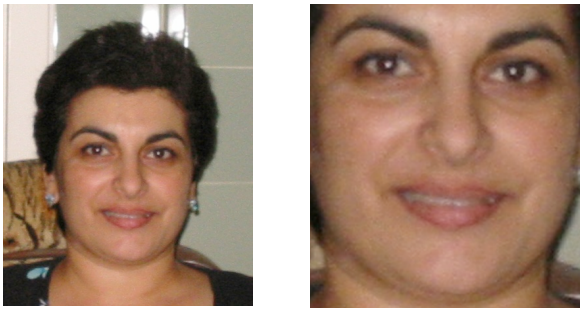

A B

Figure 2.2: Original (A) and cropped (B) images from FGNET database

Some of the images need more modification for example in FG-NET database. On the other hand, some of the faces are in a position that eyes are not in the same direction. Therefore it is necessary to locate the eyes on the same line of coordinates (Figure 2.3). For cropping and rotating images Torchvision [33] program is used, which is a machine vision library, written in simple C++ programming language and based on the Torch machine-learning library.

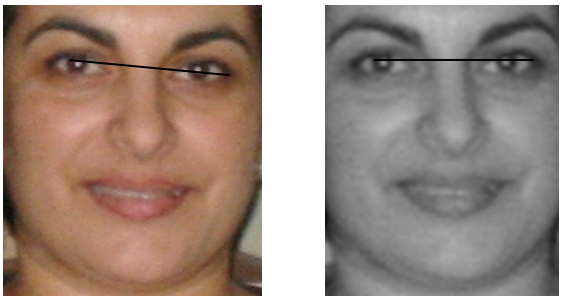

Figure 2.3: Original and rotated image

2.2 Resizing and Interpolation of Images

Each image that is given to the algorithm as an input may have different size therefore in this step it is necessary to unify size of all images. In our work, in order to resize the images, interpolation techniques had been used. Interpolation means resizing images by using known data to estimate values at known location. There are three types of interpolation such as nearest neighbor interpolation, bilinear interpolation and bicubic interpolation. In this thesis, bicubic interpolation which is the most efficient method among interpolation techniques has been used. Bicubic interpolation uses 16 nearest neighbors of new location to estimate the intensity level of it. Bicubic interpolation preserves detail of image better than the other interpolation methods.

2.3 Histogram Equalization

Histogram in image processing represents the relative frequency of occurrence of various gray levels in the image. Images may have different number of intensity levels, congestion of intensities in different levels might be different and these differences among images will decrease the efficiency of facial age classification.

In the same database the intensity levels of two images might be different. In order to distribute their levels of intensities, histogram equalization (HE) technique can be

used. HE increases the range of intensity and spreads the intensity distributions which are better than having flattened peaks and valleys for an image in terms of a histogram [11]. This operation increases contrast of the low contrast areas without affecting the overall contrast of the image.

Histogram equalization technique increases the facial age classification rate by equalizing the levels of intensities of different images that should be equalized as much as possible. Implementing the histogram equalization technique almost equalizes the distribution of intensity levels in different images. Figure 2.4 and 2.5 show the images and histograms before and after using the histogram equalization (HE) technique.

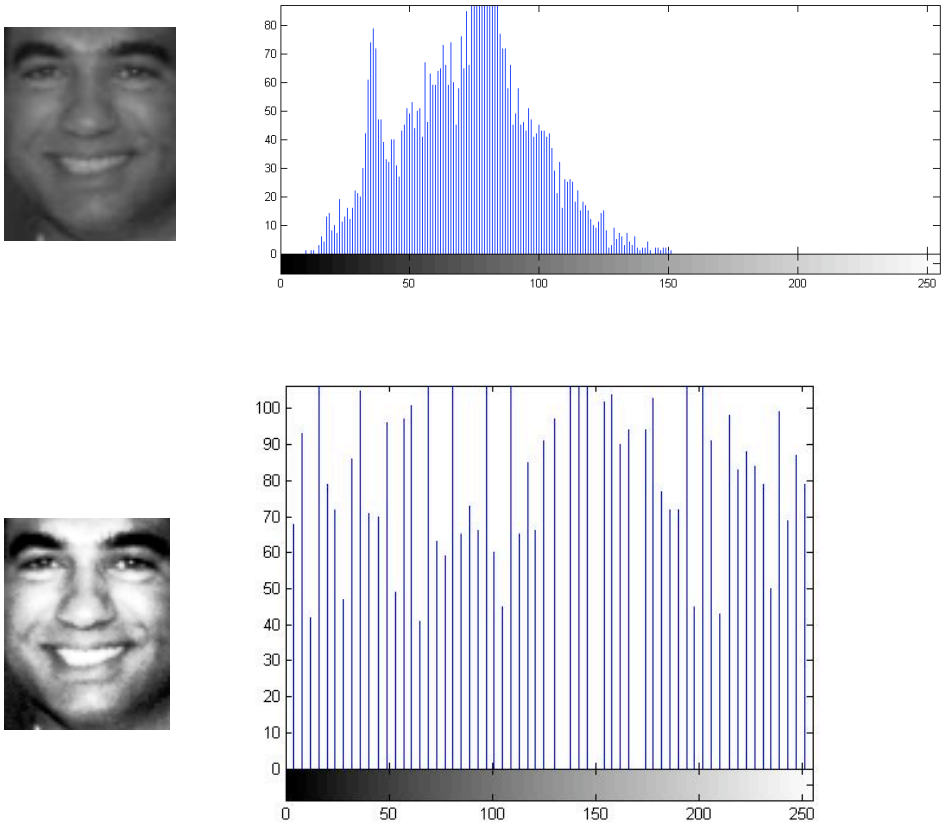

Figure 2.4: Histograms of dark image before and after histogram equalization

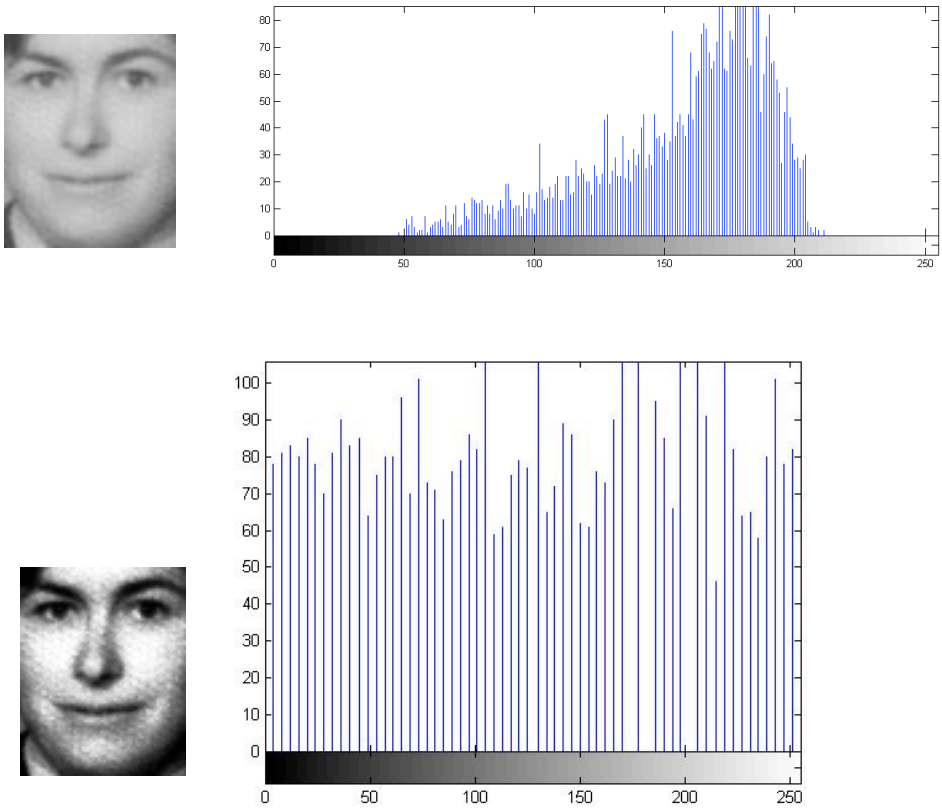

Figure 2.5: Histograms of bright image before and after histogram equalization

As Figure 2.4 and 2.5 indicates, distribution of intensity level of both images is almost close to each other. Figure 2.6 shows the differences between images before and after applying HE techniques. Contrast of both images after implementing HE techniques is close to each other. For example, image A initially was dark and after applying HE techniques become lighter or image B initially was light and after HE technique it becomes darker.

Figure 2.6: Sample images before (A & B) and after (C & D) histogram equalization

Histogram equalization is obtained by the following mathematical formula

$$S_K = (L-1)\sum_{j=0}^{k} P_{r(rj)}$$

where L is the total number of possible intensity levels, k = 0, 1, 2, …, L – 1 and P_r is the estimate of the probability of occurrence of intensity level in an image. Histogram equalization is a function of rounded S_k and n_k where n_k is number of pixels that have intensity value r_j, where r_j is the intensity level of input image.

2.4 Mean-Variance Normalization

Mean and variance normalization technique (MVN) is commonly used to increase the robustness of recognition features [12]. Feature normalization techniques are able to largely reduce the actual mismatch between training and testing conditions. Both histogram equalization (HE) and mean and variance normalization (MVN) [13] have been used to process feature vectors in order to significantly improve the classification performance.

MVN is obtained as follows:

$$R = X - M_x \, , \; MVN = R \, / \, std \, (R)$$

where X is a matrix consisting of the intensity values of a grayscale image, $M_x$is mean value of X and std is standard deviation of R.

In the study, after these steps are done, preprocessing on the facial images were finished and the images become ready to enter into training and testing parts of the feature extraction techniques (LBP, mPCA, PCA and ssLDA), which will be explained in the next chapter.

Chapter 3

FEATURE EXTRACTION

Adult faces contain lots of wrinkles and other skin artifacts known as face features which are the essential component of a successful biometrics classification algorithm; therefore accuracy of feature extraction is important to detect the age of facial image. For this purpose, facial images are used for the classification of age groups and the classification is done using Local Binary Patterns (LBP), modular Principal Component Analysis (mPCA), Principal component analysis (PCA) and subspace Linear Discriminant Analysis (ssLDA) statistical approaches for texture analysis.

One way to achieve the texture classification in gray scale images is to use the LBP texture descriptors to build several local descriptions of the facial image and concatenate them into a global description. The LBP operator [14] is one of the best performing texture descriptors and it has been widely used in various applications.
The rational behind mPCA is same as rational behind LBP, face images were divided into smaller regions in mPCA and LBP, the difference is the weight vectors that are computed for each of these regions. The weights are more representative of the local information of the face in mPCA while LBP concerns the binary number of each region and the histogram of the labels can be used as a texture descriptor for each region. These local feature based methods are more robust against variations in pose

or illumination than holistic methods. Holistic description of a face is not reasonable since texture descriptors tend to average over the image area [15, 16].

PCA projects images into a subspace such that the first orthogonal dimension of this subspace captures the greatest amount of variance among the images and the last dimension of this subspace captures the least amount of variance among the images [23, 24]. In this respect, the eigenvectors of the covariance matrix are computed which correspond to the directions of the principal components of the original data and their statistical significance is given by their corresponding eigenvalues.

While PCA tries to generalize the input data by dimension reduction, LDA tries to discriminate the input data by dimension reduction. LDA [17, 18] searches for the best projection to project the input data on a lower dimensional space in which the patterns are discriminated as much as possible. For this purpose, LDA tries to maximize the scatter between different classes and minimize the scatter between the input data in the same class. In subspace LDA [18], PCA is used for the purpose of dimension reduction by generalizing the data and LDA is used for classification due to its discrimination power. Subspace LDA method is simply the implementation of PCA by projecting the data onto the eigenspace and then implementing LDA to classify the eigenspace projected data.

In this study, we mainly used LBP and mPCA, original PCA and subspace LDA methods for feature extraction on the facial images, then classification strategy is used to obtain the classification accuracy of the methods. The results obtained by LBP method with several parameter values were compared with the results using mPCA, PCA and ssLDA methods.

3.1 Subpattern-based Approaches

Subpattern-based approaches are partitioning the images into equal-width non-overlapped regions and then extract the local features from each of these regions using Local Binary Pattern and modular Principal Component Analysis. The extracted local features correspond to the local projection, which are finally synthesized into a global feature of the original whole image for subsequent classification. The global features corresponding to the training image projections are compared with the test image projections using Manhattan and Chi Squared distance measures to detect the facial images' ages. Subpattern-based approaches are implemented in this study with different number of regions as shown in Figure 3.1.

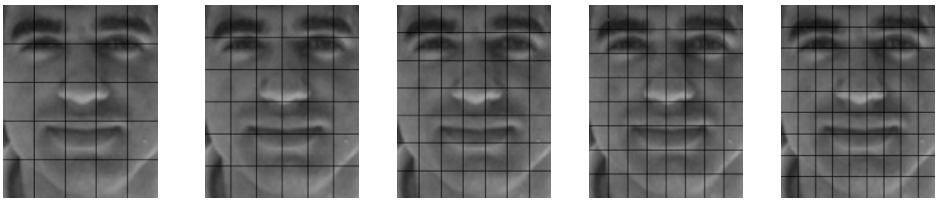

Figure 3.1: Examples of facial images with different number of regions (25, 36, 49, 64, 81 partitions)

3.1.1 Local Binary Patterns (LBP)

LBP is a texture descriptor which codifies local primitives such as (curved edges, spots, flat areas, etc) into a feature histogram. LBP based face description proposed by Ahonen et al. in 2006, stated that the facial image is divided into local regions and LBP texture descriptors are extracted from each region independently. The descriptors are then concatenated to form a global description of the face.

In order to build local descriptions, LBP extract the features from the image by assigning the labels into the pixels in a way that by thresholding pixels in a certain

neighborhood with the center value. LBP construct the code for every pixel and considers the result as a binary number. The occurrence histogram of these labels is used as texture features or descriptors. Finally different histograms can be combined as a code image.

To be able to deal with textures at different scales, the LBP operator was later extended to use neighborhoods of different sizes [16]. A circular neighborhood and bilinearly interpolating values at non-integer pixel coordinates allow any radius and number of pixels in the neighborhood. Figure.3.2 demonstrates an example of circular neighborhoods.

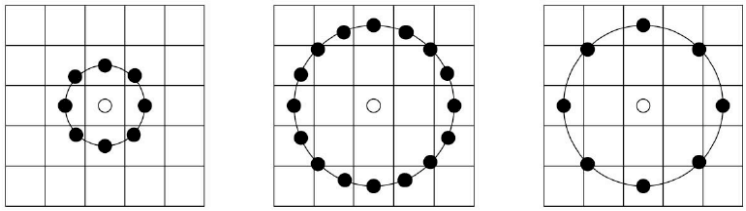

a) p = 8, r = 1 b) p = 16, r = 2 c) p = 8, r = 2

Figure 3.2: Example of circular neighborhoods.

3.1.1.1 Local Binary Patterns (LBP) Algorithm

Three different levels of locality can be applied to have a description of the face:

The LBP labels for the histogram contain information about the patterns on a pixel-level, the labels are summed over a small region to produce information on a regional level; the regional histograms are concatenated to build a global description of the face [15].

The LBP code construction steps for every pixel are as follows:

Step 1: assume that the image size is 64x80 pixels (metrics contains the pixel values of 64 rows and 80 columns), in order to divide the image into regions. At first, if 5*5 is the number of selected regions, the image should be divisible by 5, after resizing the image (resized image size is 60x80), then it is ready to split the image into 5*5 blocks so that each region contains 12*16 pixels. In Figure 3.1, different number of rectangular regions are demonstrated. The regions do not need to be rectangular or cover the whole image part, but it can be circular region which located in fiducial points as shown in Figure.3.2.

Step 2: Block processing will apply on each region separately. It is needed to assign the label to each pixel in corresponding region. Center pixel, number of neighbor pixels and radius of region are defined. If the pixel value of neighbors are bigger than the center pixel value, the label is 1; otherwise it is 0. So that each pixel of the region is labeled as

$$LBP_{(p,r)}(X_c) = \sum_{p}^{p-1} u(X_p - X_c)2^p \tag{3.1}$$

$$u_y = \begin{cases} 1, & y \geq 0 \\ 0, & y < 0 \end{cases}$$

where X_c is the pixel value of center point, X_p pixel value of sample point. The notation (p,r) will be used for pixel neighborhoods where p is the number of sampling points on a circle of radius of r. The calculation is depicted graphically in Figures 3.3 and 3.4

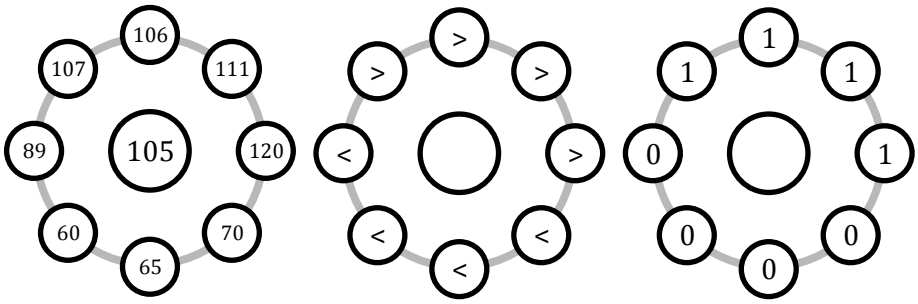

Figure 3.3: An example of LBP computation

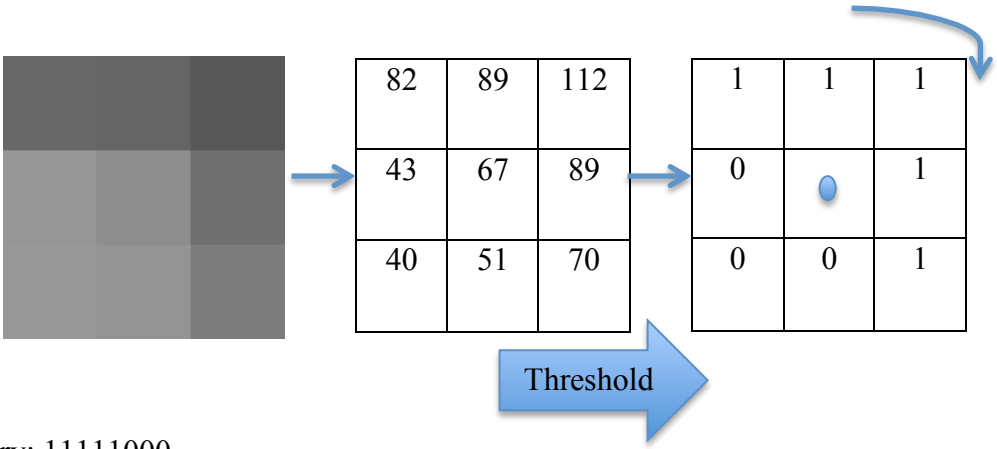

Binary: 11111000

Decimal: $(11111000)_2 = 248$

Figures 3.4: The basic LBP operator

The definition of uniform patterns is another extension of LBP. In other words, uniform pattern can be used to reduce the length of feature vector size and by implementing the simple rotation-invariant descriptor it can achieve to uniform pattern. An example of uniform pattern can be explained in a simple way as follows;

00000000	0 transitions	uniform patterns
00011110	2 transitions	uniform patterns
11001111	2 transitions	uniform patterns
11001001	4 transitions	non-uniform patterns
01010010	6 transitions	non-uniform patterns

Step3: Spatially enhanced histogram is needed in order to obtain LBP histogram. In the spatially enhanced histogram, the LBP labels for the histogram contain information about the patterns on a pixel-level which is explained in step 2. The labels are summed over a region to produce information on a regional level, and each region has a histogram itself so histograms are concatenated to build a global description of the face. Therefore, LBP histogram can be used as a texture descriptor. Figure 3.5 shows samples of enhanced histogram of image and image code before and after applying LBP is depicted in Figure 3.6.

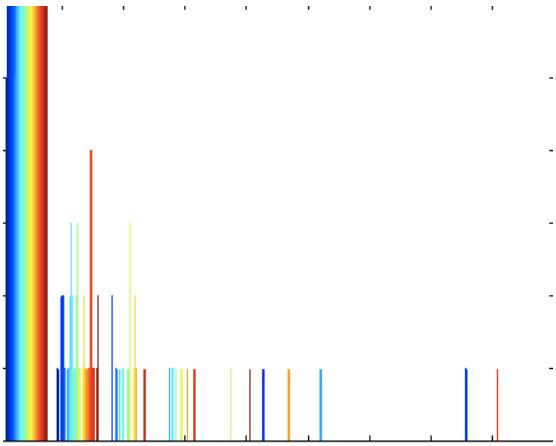

Figure 3.5: Histogram of image after concatenating all histograms

a b

Figure 3.6: a) Original Image, b) LBP Image

In this thesis we used Local Binary Patterns (LBP) histograms and Chi Square as dissimilarity measure to find the system classification.

Chi Square distance [19] is a metric in which the distance between two vectors is

$$D_{(X,\ Y)} = \chi^2 = \sum_{i=1}^{n} \frac{(x_i - y_i)^2}{x_i + y_i}$$

where X and Y are vectors of length n.

3.1.2 Modular Principal Component Analysis (mPCA)

Modular PCA method is an extension of the conventional PCA method. In modular Principle Component Analysis (mPCA), an image is first partitioned into several smaller regions and the weight vectors are computed for each of these regions which will be more representative of the local information. Then a single conventional PCA is applied to each of these regions, and therefore, the variations in the image, such as illumination and pose variations, will only affect some regions in mPCA rather than the whole image in PCA [20]. In other word, modular Principal Component Analysis (mPCA) overcomes the difficulties of regular PCA. Generally, conventional PCA considers the global information of each image and represents them with a set of weights. Under these conditions the weight vectors will vary considerably from the weight vectors of the images with normal pose and illumination, hence it is difficult to identify them correctly. On the other hand, mPCA method applies PCA on smaller regions and the weight vectors are calculated for each of them, so local information of the image can show the weights better and for variation in the pose or illumination, only some of the regions will vary and the rest of the regions will remain the same as the regions of a normal image [21].

3.1.2.1 Modular Principal Component Analysis (mPCA) Algorithm

The first step of image classification by mPCA algorithm [21] after collecting I_i images (I_i= [I_1, I_2..., I_M]) is dividing each image in the training set into N smaller images. The average image of all the training sub-images is calculated using equation (3.2). Equation (3.3) shows normalizing each training sub-image by subtracting it

from the mean. Then covariance matrix can be computed from the normalized sub-images using equation (3.4). Finding the eigenvectors $(E_1,\ E_2, \dots, E_{M'})$ of covariance matrix that are associated with the M' largest eigenvalues is the next step in which the eigenvectors according to their corresponding eigenvalues from high to low are ordered. Then the projection of training sub-images is computed in equation (3-5) using the eigenvectors.

$$A = \frac{1}{M.N} \sum_{i=1}^{M} \sum_{j=1}^{N} I_{ij} \tag{3.2}$$

$$Y_{ij} = I_{ij} - A \qquad \forall_{i,j} \tag{3.3}$$

$$C = \frac{1}{M.N} \sum_{i=1}^{M} \sum_{j=1}^{N} Y_{ij}.Y_{ij}^{T} \tag{3.4}$$

$$W_{pnjK} = E_K^T.\left(I_{pnj} - A\right) \forall_{p,n,j,k} \tag{3.5}$$

The last step of classifying images by mPCA algorithm is finding the projection for the test sub-images into the same eigenspace according to equation (3.6). The projected test sub-image is compared to every projected training sub-image and the training image that is found to be closest to the test image is used to identify the training image.

$$W_{testjK} = E_K^T.\left(I_{testj} - A\right) \forall_{j,k} \tag{3.6}$$

3.2 Holistic Approaches

Holistic or appearance based approaches deal with the entire image, not some specific features or some smaller parts. While analyzing the whole face, it tries to match templates and with the global representations, it is aimed to identify faces [22]. To take the whole image as one, and work on it means the following; there will be only one matrix with one dimension composed of all pixels in the image and all the information in the image will be kept and processed. This can be both

advantageous and disadvantageous. It is our benefit to have any information about the person to discriminate them from the others, where in a feature-based approach this is not possible, but also there may be unwanted data in the image like a wall, tree or some other items' parts rather than person's face in the background of an image. If the second case is present, of course this will affect the performance of the face classification system. As an example, in Figure 3.7-a, there are no background items, after cropping the whole face, every pixel will be useful to discriminate from others; but in Figure 3.7-b,c,d, we have some items like checked surface near the cheek, and also the part of a shirt on the bottom, which will be analyzed as well during the process of classification and will mislead the algorithm that is used.

a b c d

Figure 3.7: Samples of cropped facial images

A one-dimensional matrix composed of every pixel of the image, can be huge in size, so it is hard to be analyzed by a machine. The two popular statistical dimensionality reduction methods, PCA and subspace LDA can be used in a holistic manner, where they extract features from the whole face image, reduce the size and then classify them accordingly again considering the whole image.

For this purpose, statistical dimensionality reduction methods such as Principal Component Analysis (PCA) and Linear Discriminant Analysis (LDA) are

demonstrated to be successful in several academic studies and commercial applications. The success and popularity of these algorithms are mainly due to their statistics-based ability of automatically deriving the features instead of relying on humans for their definitions. In the next two sections PCA and subspace LDA methods are explained in detail.

3.2.1 Principal Component Analysis (PCA)

Principal Component Analysis (PCA) [23] is one of the most common techniques to reduce the number of dimensionality, which makes this in a very efficient way, making PCA successful and popular. PCA is efficient, because the algorithm achieves its job with only a simple linear algebra and without much loss in the data.

Before describing the PCA, it is important to define eigenvectors in mathematical terms as it is important part of this algorithm. The mathematical definition of eigenvector can be defined as AC=C, where A is a square matrix, C is the eigenvector of A and it is not a zero vector, and real or complex must be present. Eigenvectors can be only found for square matrices but not every square matrix has them. And if it does, and the square matrix has the dimension m x m, then there are m eigenvectors. The important property of eigenvector is that when we multiply it with a vector, it only makes it longer; it does not change its direction.

When we reconsider PCA with mathematical terms, we can say that it projects images into a subspace such that the first orthogonal dimension of this subspace captures the greatest amount of variance among the images and the last dimension of this subspace captures the least amount of variance among the images [23, 24, 25]. In this respect, the eigenvectors of the covariance matrix are computed which

correspond to the directions of the principal components of the original data and their statistical significance is given by their corresponding eigenvalues.

3.2.1.1 Principal Component Analysis (PCA) Algorithm

The PCA algorithm can be stated as follows;

Step 1: Take the all images (xi) into a row of vectors of size V: xi = [xi1 … xi v], where V is the total numbers of pixels in an image.

Step 2: Subtract the Mean: Calculate the mean m, which equals sum of all training images divided by the number of them, and subtract it from of x;

$$m = \left(\sum_{i=0}^{n} x^{i}\right) * 1/N \tag{3.7}$$

$$y^{i} = x^{i} - m \tag{3.8}$$

Step 3: Create the data matrix by combining the above vectors; $Z = \left[y_1^i \ldots y_v^i\right]$

Step 4: Calculate the covariance matrix:

$$C = ZZ^{T} \tag{3.9}$$

Step 5: Determine the eigenvalues of covariance matrix C.

Step 6: Sort the eigenvalues (and corresponding eigenvectors) in decreasing order.

Step 7: Assume that $N \leq V$, select the first $d \leq R$ eigenvectors and generate the dataset in the new representation.

Step 8: Compare the test image's projection matrix with the projection matrix of each training image by using a similarity measure. The result is the training image which is the closest to the test image.

3.2.2 Subspace Linear Discriminant Analysis (ssLDA)

Linear Discriminant Analysis [24] is a method that in which statistical and supervised machine learning techniques are used to classify the unknown classes in test sample based on known classes in training samples. LDA is used to project the samples from the high dimensional space to a lower dimensional feature space.

Maximize between class variance and minimize the within class variance are the aims of LDA to find the most discriminant projection direction. Figure.3.8 shows an example of 3 age intervals classified using LDA.

In this study, for the first step of classification, 3 classes are defined in 3 age intervals as 0-20, 21-40 and 41-60 as shown in Figure 3.8. The first row images belong to 0 to 20 years old, second row images belong to 21 to 40 and third row images belong to 41 to 60 years old human beings. Large variance between classes and small variance within classes is obvious.

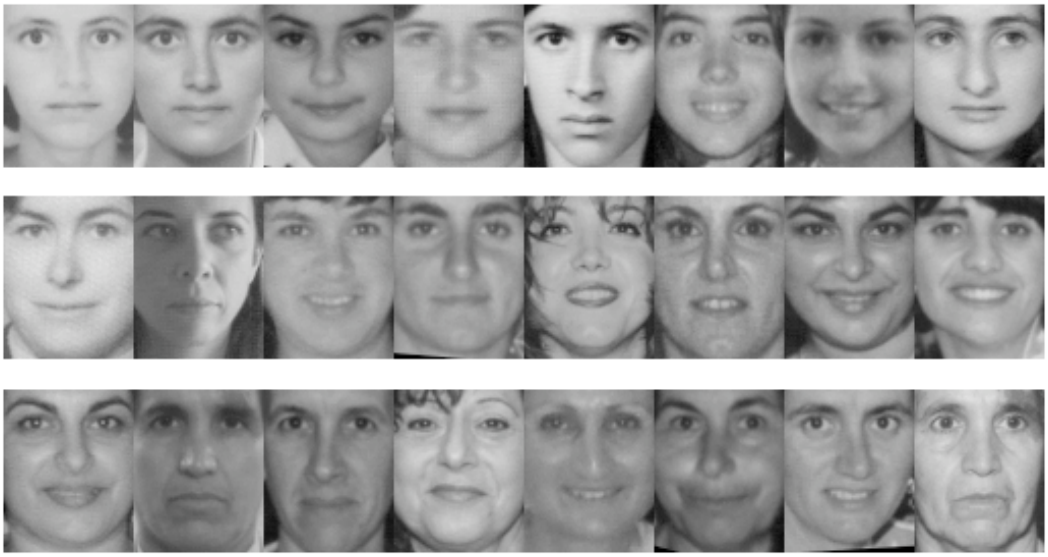

Figure 3.8: Facial images of three different age intervals selected from FG-NET aging database

Subspace LDA method is simply the implementation of PCA by projecting the data onto the eigenspace and then implementing LDA to classify the eigenspace projected data. Within class scatter matrix measures the amount of scatter between items in the same class. For the *ith* class, a scatter matrix (Si) is calculated as the sum of the covariance matrices of the centered images in that class as follows

$$S_i = \sum_{x \in X_i} (x - m_i)(x - m_i)^T \quad (3.10)$$

where m_i is the mean of the images in the class. The within class scatter matrix (S_W) is the sum of all the scatter matrices. Here $X_i$is the projection constructed from PCA algorithm. $S_W$is calculated as

$$S_W = \sum_{i=1}^{L} S_i \quad (3.11)$$

where *L* is the number of classes.

Equation (3.12) shows the between classes scatter matrix (S_B) which measures the amount of scatter between classes. It is calculated as the sum of the covariance matrices of the difference between the total mean and the mean of each class as follows

$$S_B = \sum_{i=1}^{C} n_i(m_i - m)(m_i - m)^T \quad (3.12)$$

where n_i is the number of images in the class, $m_i$is the mean of the images in the class and m is the mean of all the images.

3.2.2.1 Subspace Linear Discriminent Analysis (ssLDA) Algorithm

Subspace Linear Discriminant Analysis (ssLDA) algorithm can be stated as follows:

Step 1: Take all the images (x^i) into a row vector of size V: $x^i = \left[x_1^i \dots x_v^i\right]$

Step 2: Subtract the Mean: Calculate the mean *m,* which equals sum of all training images divided by the number of them, and subtract it from all the images (x);

$$m = \left(\sum_{i=0}^{n} x^i\right) * 1/N \quad (3.13)$$

$$y^i = x^i - m \quad (3.14)$$

Step 3: Create the data matrix by combining the above vectors; Z = $\left[y_1^i \dots y_v^i\right]$

Step 4: Calculate the covariance matrix:

$$C = ZZ^T \quad (3.15)$$

Step 5: Determine the eigenvalues of covariance matrix C

Step 6: Sort the eigenvalues (and corresponding eigenvectors) in decreasing order.

Step 7: Assume that $N \leq V$, select the first $d \leq R$ eigenvectors and generate the dataset in the new representation.

Step 8: Take the projection from the PCA as an input to LDA, X_i

Step 9: Calculate within-class scatter matrix, S_W of X.

Step 10: Calculate between-class scatter matrix, S_B.

Step 11: Calculate the eigenvectors of the projection matrix:

$$W = eig(S_W^{-1} S_b) \tag{3.16}$$

Step 12: Compare the test image's projection matrix with the projection matrix of each training image by using a similarity measure. The result is the training image which is the closest to the test image.

In this study the Manhattan distance is used for PCA and ssLDA as similarity measure. Manhattan Distance is a metric in which the distance between two points is the sum of the (absolute) differences of their coordinates. It is also known as rectilinear distance, L1 distance or city block distance.

The Manhattan distance between the point P1 with coordinates (x1; y1) and the point P2 at (x2; y2) is:

$$D_{Manhattan} = |x_1 - x_2| + |y_1 - y_2|$$

and Manhattan distance between two vectors X, Y of length n is [19]:

$$D_{(X,\ Y)} = \sum_{i=1}^{n} |x_i - y_i|$$

Chapter 4

GEOMETRY ANALYSIS

4.1 Geometric Variation

Age estimates are obtained from faces whose shape and degree of skin wrinkling are changed. Both of the variables affect the perceived age of faces. [26]. Therefore, focus on the contributions of shape-based features and texture-based features in age estimation or classification from facial images is needed. Facial shape variations are more visible during babyhoods, on the other hand it becomes subtle during adulthood. Hence, facial aging can be described as a problem of characterizing facial shape and facial texture as functions of time [8].

Infant faces have lots of wrinkles and it is not suitable to just extract the texture features of babies but since the structure of head bones in infanthood is not full-grown and the ratios between primary features (e.g. distance between eyes, face width, length, thickness of nose, etc.) are different from those in other life periods, using the geometric relations of primary features is more reliable than wrinkles when an image is judged to be a baby or not.

In this thesis, LBP, mPCA, PCA and ssLDA operators are used for texture analysis as it is discussed before in chapter 3. In this chapter the geometric features of facial images and geometric variation in babies versus adults are considered. In Figure 4.1, the variation of distance between primary features from childhood to adulthood is demonstrated.

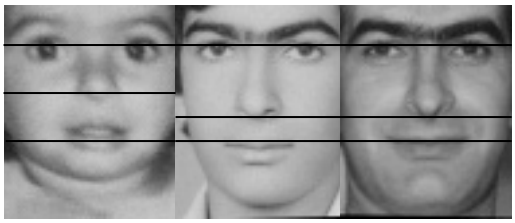

a: 2 years old, b: 16 years old, c: 29 years old

a: 1 years old, b: 22 years old, c: 45 years old

Figure 4.1: Variation of distance between primary features

4.2 Ratio Analysis

Kwon and Lobo [2] classified ages from facial images into 3 age groups as babies, young adults and senior adults. They used cranio-facial development theory and skin wrinkle analysis in their study. Using the primary features of the human face such as eyes, nose, mouth, chin and virtual top of the head; mainly 6 different ratios are calculated to distinguish babies from young adults and senior adults. Then they used secondary feature analysis with a wrinkle geography map to detect and measure wrinkles to distinguish seniors from babies and young adults. Finally, they combined ratios and wrinkle information obtained from facial images to classify faces into 3 age groups.

From these primary features, geometric ratios are computed. Figure 4.2 graphically explains these ratios.

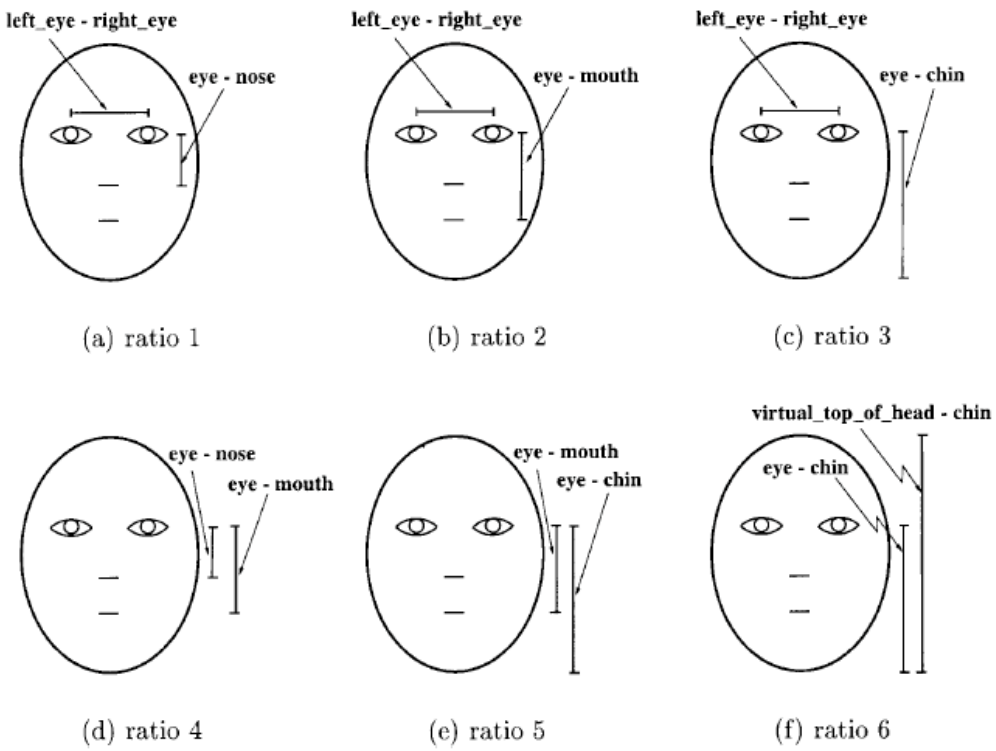

Figure 4.2: Six different ratios [2].

In babyhood, the head is near a circle. The distance from eyes to mouth is close to that between two eyes. With the growth of the head bone, the head becomes oval, and the distance from the eyes to the mouth becomes longer. Besides, the ratio of the distance between babies' eyes and noses and that between noses and mouths is close to one, while that of adults' is larger than one, as illustrated in Figures 4.1 (a) and (b, c). Therefore, two geometric features are defined below for recognizing babies.

4.2.1 Algorithm Using Ratio Analysis

The algorithm is as follows:

Step 1: Locating the primary features is very important step in extraction of features, and it can be automatically or manually. Wen-Bing Horng et. al [27] automatically located the primary features in their study. First of all central horizontal line of the image is found, then they found the eyes location, and finally nose and mouth

location is found. Am_markup tools also can let the researcher to locate the features manually. In this study we used am_markup tools [28] to locate the points in only MORPH database, since the features are publicly available in FG-NET database. Figure 4.3 illustrates a sample image in FG-NET in which the features are located and labeled.

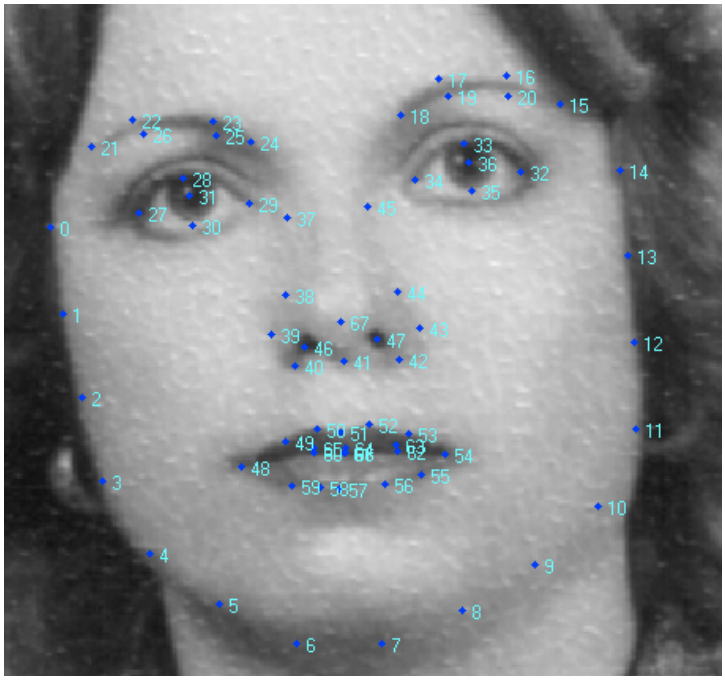

Figure 4.3: FGNET facial image with located and labeled feature points

Step 2: Find the distance between the primary features.

Step 3: Find the ratios as follows

The first geometric feature is defined as

$$R_{em} = \frac{D_{em}}{D_{ee}} \qquad (4.1)\ [27]$$

where D_{em} is the distance between the eyes and the mouth, and D_{ee} is the distance between two eyes' iris. R_{em} in babies smaller than R_{em} in adults, because the baby's faces is near a circle so R_{em} in adults becomes larger.

Second geometric feature is

$$R_{enm} = \frac{D_{en}}{D_{nm}} \quad (4.2)\ [27]$$

where D_{en} is the distance between the eyes and the nose, and D_{nm} is the distance between the nose and the mouth. The distance between the eyes and the nose of a baby is smaller than the distance between the eyes and the nose of an adult, so the value of R_{enm} becomes larger in adult faces. The values of these two ratios are used to recognize babies in the experiments on the next chapter.

Chapter 5

EXPERIMENTS AND RESULTS

Together with preprocessing techniques, holistic and subpattern-based approaches are used to classify the ages via facial images. The experiments are performed using FGNET [29] and MORPH [30] aging databases in three different categories for evaluating the performance of subpattern-based approaches (LBP and mPCA) and holistic approaches (PCA and ssLDA).

In the experiments for the holistic approaches, all the training and test images used are cropped and scaled down to 64x80 pixels from the original sizes, so that they only include the head of the individuals that is explained in detail in Chapter 2. For the subpattern-based approaches, in order to divide the images to equal size with proper values, the images are resized to 78x63, 80x60, 78x60, 77x63, 72x63, 80x60, 77x55, 72x60 pixels for 9, 25, 36, 49, 81, 100, 121 and 144 subpatterns respectively. Three datasets are selected from FG-NET and MORPH databases which include at least three samples for each individual.

For the comparison of the training image and test image projections which are the results of feature extraction algorithms, they are compared with Manhattan distance measure and Chi squared distance measure [19] to classify the face images according to the corresponding age. For calculating this measure, test image projections are subtracted from the training image projections and for each person's projection, the

absolute differences are summed. The smallest difference is the one found by the algorithm which is chosen as the closest age for that test image. Classification accuracy for a set of images is computed as the ratio of the number of images correctly classified using holistic and subpattern-based approaches to the number of total test images in the set.

5.1 Description of Databases

5.1.1 FG-NET Aging Database

FG-NET is a large and the publicly available aging database. FG-NET database contains 1002 images of 82 individuals at different ages with color and grey scale face images. The images of FG-NET display significant variability in resolution, quality, illumination and expression since the database images are collected by scanning the photographs of subjects found in personal collections [29]. In this study, we used frontal images of female and male subjects with free of glasses, beard and mustache, all samples are taken from different ages. The age differences between the selected image samples are in the range 0 - 60 years. In this study, a subset of this database (750 images) is selected according to the ages of subjects.

5.1.2 MORPH Aging Database

MORPH database is a longitudinal aging database which contains 1724 images of 515 subjects. There are approximately 3 images per subject with different ages. MORPH database images include age, gender and ethnicity information. Some of the subjects with 3 frontal images at different ages from MORPH database are selected in this thesis to perform the experiments. The age differences between the selected image samples are in the range 2 months - 60 years. In this study, a subset of this database (320 images) is selected according to the ages of the images. MORPH database images include age, gender and ethnicity information. Some of the subjects

with 3 frontal images at different ages from MORPH database are selected in this study to perform the experiments. The age differences between the selected image samples are in the range of 2 months to 60 years.

Moreover, two main steps exist in order to classify facial images. Training phase is the first step in which first of all a dataset of normalized images are given to the feature extraction algorithm then projection of train images is obtained as an output of training phase. Similarly, in test phase, normalized test image will be projected to the subspace of training phase and then the new projection of test images is available to be compared with projected training images. The steps are depicted in Figures 5.1, 5.2 and 5.3. Classification step is done after the test phase in which comparison between projected test images and projected training images is performed using Manhattan distance and Chi Squared distance.

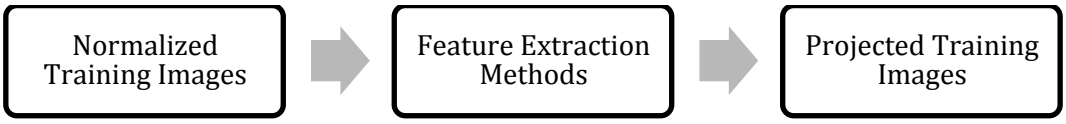

Figure 5.1: Training phase steps

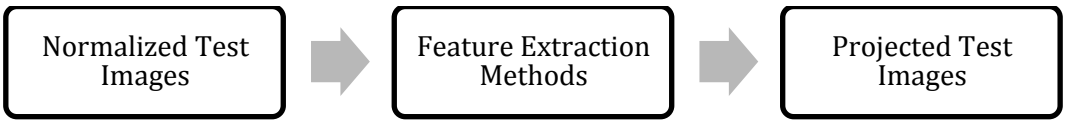

Figure 5.2: Test phase steps

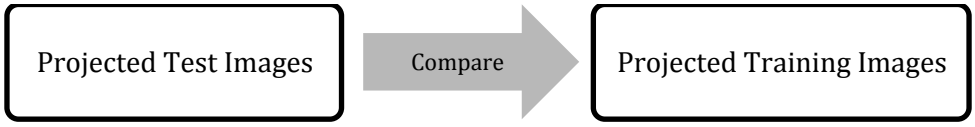

Figure 5.3: Classification step

5.2 First Step Age Classification Experiments on facial images

First step age classification experiments of facial images are done on three subsets of FG-NET and MORPH databases by categorizing them into 3 different age intervals. The facial images used in the experiments range from 0 to 60 years and the ages are classified into 3 categories for the age ranges of 0-20 years, 21-40 years and 41 to 60 years. Each dataset includes 3 classes; in FG-NET 540 images are used for training and 205 for the test. 250 and 70 images are used for training and test phase respectively in MORPH subset and in the combination of FGNET and MORPH subset, 667 images are used in training phase and 275 images for test phase. More details on the number of training images and test images in each class is shown in Table 5.1.

Table 5.1:Number of training and test images in 3 subsets

FGNET								
Gender	**Training**	0-20	21-40	41-60	**Test**	0-20	21-40	41-60
Female	221	158	50	13	98	76	17	5
Male	324	260	53	11	107	86	17	4
MORPH								
Gender	**Training**	0-20	21-40	41-60	**Test**	0-20	21-40	41-60
Female	95	24	68	3	34	9	23	2
Male	155	104	49	2	36	19	16	1
FGNET+ MORPH								
Gender	**Training**	0-20	21-40	41-60	**Test**	0-20	21-40	41-60
Female	292	158	118	16	132	85	40	7
Male	375	260	102	13	143	105	33	5

5.2.1 Experiments Using Subpattern-based Approaches

Local Binary Pattern and Modular Principal Component Analysis are used as subpattern-based approaches in order to classify the images according to the corresponding ages into 3 categories. For all the tables below, the results are in (%) for the classification rates.

5.2.1.1 Experiments Using LBP

This set of experiments is done with different subpattern sizes and neighborhood values using LBP. The facial images from all subsets of the aging databases are divided into 9, 16, 25, 36, 49, 64 , 81, 100, 121 and 144 subpatterns. Local Binary Pattern histograms are extracted and concatenated into one feature histogram to represent the whole image. Age classification using (1,8), (2,8), (1,16) and (2,16) neighborhoods with uniform pattern is performed for female and male facial images. The overall age classification performances for 3 different datasets of facial images are presented in Tables 5.2-5.7. We used a nearest neighbor classifier and Chi Square distance metrics for all LBP age classification experiments in this study.

Table 5.2: Female Age Classification Rates (%) with LBP on FGNET dataset

Subpattern size	Neighborhood			
	(1,8)	(2,8)	(1,16)	(2,16)
3x3	70.40	71.42	75.51	81.63
4x4	72.44	70.40	78.57	74.48
5x5	71.42	74.48	75.51	77.55
6x6	74.48	83.67	79.59	78.57
7x7	75.51	77.55	79.59	78.57
8x8	80.61	80.61	80.61	82.65
9x9	81.63	75.51	76.53	76.53
10x10	79.59	78.57	80.61	77.55
11x11	77.55	79.59	79.59	73.46
12x12	81.63	82.65	80.61	79.59

LBP female age classification results with different subpattern sizes and neighborhoods are different on FGNET dataset. In addition, female age classification results demonstrate that female age classification using 36 (6x6) subpatterns and (2, 8) neighborhoods shows better classification rate witch is 83.67%. On the other hand, female age classification using (1, 8) neighborhood and 9 subpatterns achieves the minimum result which is 70.40%. In other words, LBP female age classification using 36 subpatterns and (2, 8) neighborhoods is around 13% better than female age classification using 9 subpatterns with (1, 8) neighborhoods on FGNET dataset.

Table 5.3: Female Age Classification Rates (%) with LBP on MORPH dataset

Subpattern size	Neighborhood			
	(1,8)	(2,8)	(1,16)	(2,16)
3x3	55.88	64.70	58.82	64.70
4x4	67.64	70.58	64.70	61.76
5x5	55.88	58.82	50.00	61.76
6x6	61.76	64.70	64.70	67.64
7x7	61.76	58.82	58.82	47.05
8x8	67.64	70.58	61.76	55.88
9x9	58.82	44.11	50	41.17
10x10	55.88	52.94	55.88	44.11
11x11	67.64	67.64	61.76	58.82
12x12	61.76	55.88	64.70	47.05

LBP female age classification results with different subpattern sizes and neighborhoods are different on MORPH dataset. In addition, female age classification results demonstrate that female age classification using 16 (4x4) and 64 (8x8) subpatterns with (2, 8) neighborhoods show better classification rate witch is 70.58 % on MORPH dataset.

Table 5.4: Female Age Classification Rates (%) with LBP on FGNET+MORPH dataset

Subpattern size	Neighborhood			
	(1,8)	(2,8)	(1,16)	(2,16)
3x3	67.42	68.93	71.21	73.48
4x4	65.90	66.66	71.21	68.93
5x5	66.66	71.21	71.96	71.96
6x6	70.45	74.24	73.48	72.72
7x7	71.21	71.21	75.00	74.24
8x8	75.00	75.00	73.48	74.24
9x9	72.72	68.93	70.45	69.69
10x10	75	73.48	73.48	72.72
11x11	73.48	76.51	73.48	67.42
12x12	76.51	78.03	75.75	75.75

Similarly, the results of LBP female age classification on FGNET+ MORPH dataset show that the maximum rate (78.03%) is obtained with 144 subpatterns and (2, 8) neighborhoods. Moreover female age classification on FGNET is around 13% and 5% better than female age classification on MORPH and FGNET+MORPH datasets respectively.

Table 5.5: Male Age Classification Rates (%) with LBP on FGNET dataset

Subpattern size	Neighborhood			
	(1,8)	(2,8)	(1,16)	(2,16)
3x3	79.43	82.24	82.24	81.30
4x4	81.30	87.85	85.04	85.04
5x5	86.91	85.98	86.91	86.91
6x6	85.04	85.04	85.98	85.04
7x7	86.91	88.78	88.78	88.78
8x8	85.98	86.91	89.71	88.78
9x9	85.98	86.91	86.91	85.04
10x10	85.98	85.04	88.78	85.04
11x11	87.85	83.17	85.98	84.11
12x12	86.91	85.04	87.85	82.24

LBP male age classification results with different subpattern sizes and neighborhoods are presented on FGNET dataset in Table 5.5 as shown in the table, male age classification using 64 (8x8) subpatterns with (1, 16) neighborhoods shows better classification rate which is 89.71%. On the other hand, male age classification using (1, 8) neighborhood and 9 subpatterns achieves the minimum result which is 79.43%. In other words, LBP male age classification using 64 subpatterns and (1, 16) neighborhoods is around 10% better than male age classification using 9 subpatterns with (1, 8) neighborhoods on MORPH dataset.

Table 5.6: Male Age Classification Rates (%) with LBP on MORPH dataset

Subpattern size	Neighborhood			
	(1,8)	(2,8)	(1,16)	(2,16)
3x3	52.77	50.00	58.33	50.00
4x4	58.33	52.77	44.44	58.33
5x5	55.55	58.33	55.55	61.11
6x6	50.00	58.33	58.33	47.22
7x7	50.00	55.55	52.77	52.77
8x8	55.55	58.33	52.77	61.11
9x9	63.88	38.88	63.88	47.22
10x10	50.00	50	52.77	61.11
11x11	55.55	44.44	50.00	36.11
12x12	55.55	52.77	55.55	38.88

Table 5.6 shows LBP male age classification rates on MORPH dataset with different subpattern sizes. Male age classification results demonstrate that male age classification using 81 (9x9) subpatterns with (1, 8) and (1, 16) neighborhoods shows better classification rate witch is 68.88%. LBP male age classification on MORPH dataset in comparison with LBP female age classification on the same dataset, it indicates that female age classification is around 3% better than male age classification on MORPH dataset.

Table 5.7: Male Age Classification Rates (%) with LBP on FGNET+MORPH dataset

Subpattern size	Neighborhood			
	(1,8)	(2,8)	(1,16)	(2,16)
3x3	66.43	72.72	69.23	72.02
4x4	73.42	77.62	74.12	76.22
5x5	76.22	76.22	78.32	76.22
6x6	73.42	77.62	76.22	74.82
7x7	76.22	76.92	76.92	77.62
8x8	74.82	77.62	79.72	73.42
9x9	76.22	76.92	76.92	76.22
10x10	76.22	76.92	79.02	74.82
11x11	77.62	74.82	77.62	70.62
12x12	77.62	75.52	76.22	73.42

LBP female and male age classification results with different subpattern sizes and neighborhoods are presented for three datasets. In Tables 5.2-5.7 female and male age classification results demonstrate that male age classification is around 9% and 4% better than female age classification in FG-NET and combined FG-NET+MORPH datasets respectively. However female age classification is around 7% better than male age classification in MORPH database. Considering female and male age classification accuracies separately, it is observed that (2, 8) neighborhood with 64 subpatterns achieves the best results except in FG-NET dataset for females. On the other hand, for male facial images, age classification using LBP with (1, 16) neighborhood and 64 subpatterns achieves the best results expect for MORPH dataset.

5.2.1.2 Experiments Using mPCA

These experiments are done with different subpattern sizes using mPCA. The facial images from all subsets of the aging databases are divided into 4, 9, 25, 36, 49, 64 and 81 subpatterns. Modular PCA age classification using maximum number of non-zero eigenvectors is performed for female and male facial images. The overall age classification performances for 3 different datasets of facial images are presented in Tables 5.8-5.10.

Table 5.8: Female and Male Age Classification Rates (%) with mPCA on FGNET dataset

Subpattern size	Female	Male
2x2	67.34	75.70
3x3	69.38	76.63
5x5	66.32	74.76
6x6	66.32	73.83
7x7	59.18	72.89
8x8	62.24	75.70
9x9	61.22	72.89

Table 5.9: Female and Male Age Classification Rates (%) with mPCA on MORPH dataset

Subpattern size	Female	Male
2x2	47.05	61.11
3x3	52.94	58.33
5x5	55.88	58.33
6x6	55.88	61.11
7x7	58.82	58.33
8x8	50.00	58.33
9x9	58.82	58.33

Table 5.10: Female and Male Age Classification Rates (%) with mPCA on FGNET+MORPH dataset

Subpattern size	Female	Male
2x2	73.48	65.73
3x3	71.21	67.13
5x5	68.18	67.13
6x6	66.66	66.43
7x7	62.87	65.73
8x8	67.42	65.03
9x9	63.63	65.73

Modular PCA age classification results with different subpattern sizes are different for three datasets. In addition, female and male age classification results demonstrate

that male age classification is around 7% and 6% better than female age classification in FG-NET and MORPH databases respectively. However female age classification is around 6% better than male age classification in combined FGNET+MORPH database. Considering female and male age classification accuracies separately, we observe that experiment using 9 subpatterns achieve the best results except in MORPH dataset for females.

5.2.2 Experiments Using Holistic Approaches

Principal Component Analysis and subspace Linear Discriminant Analysis are used as a holistic approach in order to classify the images according to the corresponding ages into 3 categories. For all the tables, the results are in (%) for the classification rates.

5.2.2.1 Experiments Using PCA

PCA method is applied on the whole facial images using the maximum number of non-zero eigenvectors (no of images -1). The classification accuracies for age classification using PCA method are shown in Table 5.11.

Table 5.11: Female and Male Age Classification Rates (%) with PCA on 3 datasets

Dataset	Female	Male
FGNET	77.55	81.30
MORPH	58.82	50.00
FGNET+MORPH	71.21	65.73

5.2.2.2 Experiments Using ssLDA

Subspace LDA is implemented using PCA method to reduce dimensionality and then LDA method with maximum number of non-zero eigenvectors (no of classes -1) is applied. The classification accuracies for age classification using ssLDA method are shown in Table 5.12.

Table 5.12: Female and Male Age Classification Rates (%) with ssLDA on 3 datasets

Dataset	Female	Male
FGNET	74.48	88.78
MORPH	64.70	55.55
FGNET+MORPH	79.72	74.12

In the second set of experiments, the classification accuracies of LBP, mPCA, PCA and ssLDA are compared on female and male facial images as shown in Table 5.13 and 5.14. We used (2, 8) neighborhood and 64 subpatterns for female age classification and (1, 16) neighborhood and 64 subpatterns for male age classification within LBP method and 9 subpatterns for female and male age classification within mPCA method. PCA and ssLDA methods are used in the same way as explained in the previous sections. The best age classification accuracies obtained using LBP method for female and male facial images are used for comparison with mPCA, PCA and ssLDA methods. The experimental results on three different aging datasets demonstrate that LBP achieves better accuracies compared to mPCA, PCA and ssLDA accuracies for FGNET and MORPH datasets on female images. However, ssLDA performance is slightly better than LBP performance whenever the combined dataset is used. On the other hand, for male images, the classification accuracies are

consistent with the experimental results on female images. LBP method outperforms mPCA, PCA and ssLDA methods on male images of all three datasets of FGNET and MORPH.

Table 5.13: Female Age Classification with LBP, mPCA, PCA, ssLDA

Dataset	LBP	mPCA	PCA	ssLDA
FGNET	83.67	69.38	77.55	74.48
MORPH	70.58	52.94	58.82	64.70
FGNET+MORPH	75	71.21	71.21	79.72

Table 5.14: Male Age Classification with LBP, mPCA, PCA, ssLDA

Dataset	LBP	mPCA	PCA	ssLDA
FGNET	89.71	76.63	81.30	88.78
MORPH	63.88	58.33	50.00	55.55
FGNET+MORPH	79.72	67.13	65.73	74.12

5.3 Second Step Age Classification Experiments on facial images

Second step age classification experiments are done right after the first classification step by categorizing the facial images from FG-NET and MORPH databases into age ranges of 0-10, 11-20, 21-30, 31-40, 41-50 and 51-60 as second classification in order to have smaller range and more accurate age estimation. The number of images for training section is the same as the first step classification section but the number of test images is the correctly classified images in the first classification step. Therefore the number of test images is less than the first step. Second step age

classification accuracy for a set of images is computed as the ratio of the number of images correctly classified to the number of correctly classified in the first step classification. For instance if 50 images is correctly classified in class 0 to 20, the system correctly classify these 50 images into two ranges from 0 to 10 and 11 to 20 or not. If so, how would be the classification rate? The second step age classification accuracies using holistic and subpattern-based methods are demonstrated in this section.

5.3.1 Experiments Using LBP

Age classification using 36 (6x6) subpattern size and (2,8) neighborhood has better performance in the first step of classification, therefore the correctly classified test images in the first step are the test images in the second step.

The overall age classification performances for 3 different datasets of facial images are presented in Tables 5.15-5.17.

Table 5.15: Female, Male and Female+Male Second Step Age Classification Rates (%) with LBP on FGNET dataset

Gender	Dim	Classification 1	Classification 2
Female	6x6(2, 8)	83.67	68.92
Male	6x6(2, 8)	85.04	70.32
Female + Male	6x6(2, 8)	85.36	72.00

Table 5.16: Female, Male and Female+Male Second Step Age Classification Rates (%) with LBP on MORPH dataset

Gender	Dim	Classification 1	Classification 2
Female	6x6(2, 8)	64.70	72.72
Male	6x6(2, 8)	58.33	85.71
Female + Male	6x6(2, 8)	57.14	80.00

Table 5.17: Female, Male and Female+Male Second Step Age Classification Rates (%) with LBP on FGNET+MORPH dataset

Gender	Dim	Classification 1	Classification 2
Female	6x6(2, 8)	74.24	66.32
Male	6x6(2, 8)	77.62	71.17
Female + Male	6x6(2, 8)	76.36	72.38

The experimental results using LBP on three different aging datasets demonstrate that MORPH dataset has maximum accuracy in second classification in male facial images. Female, male and combined female + male second age classification results demonstrate that combined female + male age classification is around 2% and 4% better than male and female age classification in FG-NET, it is also 1% and 6% better than male and female age classification in combined FGNET+MORPH databases respectively. However, the results of FGNET and combined FGNET+MORPH are more reliable than MORPH dataset because the first step classification rate is low.

5.3.2 Experiments Using mPCA

These experiments are done with different subpattern sizes using mPCA. The facial images from all subsets of the aging databases are divided into 4, 9, 25, 36, 49, 64 and 81 subpatterns. The test images are the correctly classified images in first step classification. Modular PCA age classification using maximum number of non-zero eigenvectors is performed for female and male facial images. The overall age classification performances for 3 different datasets of facial images are presented in Tables 5.18-5.20. The following notations are used in the tables:

1: represents the first step classification performance,

2: represents the second step classification performance

Table 5.18: Female and Male Second Step Age Classification Rates (%) with mPCA on FGNET dataset

Subpattern size	Female		Male	
	1	2	1	2
2x2	67.34	51.02	75.70	60.74
3x3	69.38	53.06	76.63	58.87
5x5	66.32	52.04	74.76	54.20
6x6	66.32	51.02	73.83	54.20
7x7	59.18	50.00	72.89	55.14
8x8	62.24	47.95	75.70	57.94
9x9	61.22	46.93	72.89	55.14

Table 5.19: Female and Male Second Step Age Classification Rates (%) with mPCA on MORPH dataset

Subpattern size	Female		Male	
	1	2	1	2
2x2	47.05	38.23	61.11	52.77
3x3	52.94	35.29	58.33	50.00
5x5	55.88	41.17	58.33	47.22
6x6	55.88	44.11	61.11	47.22
7x7	58.82	38.23	58.33	47.22
8x8	50.00	35.29	58.33	47.22
9x9	58.82	41.17	58.33	47.22

Table 5.20: Female and Male Second Step Age Classification Rates (%) with mPCA on FGNET+MORPH dataset

Subpattern size	Female		Male	
	1	2	1	2
2x2	73.48	53.78	65.73	50.34
3x3	71.21	50.75	67.13	49.65
5x5	68.18	50.00	67.13	47.55
6x6	66.66	49.24	66.43	46.85
7x7	62.87	48.48	65.73	46.85
8x8	67.42	50.00	65.03	48.25
9x9	63.63	48.48	65.73	44.75

Modular PCA second age classification results with different subpattern sizes are different for three datasets. In addition, the results with 4 (2x2) and 9 (3x3) subpatterns sizes demonstrate better performance in both female and male second step classification. However, In MORPH dataset the best results is obtained using 36 (6x6) subpatterns size. In addition, male second age classification using 9 subpatterns is around 5% better than female second age classification in FGNET. However female second age classification is around 4% better than male second age classification in combined FGNET+MORPH database.

5.3.3 Experiments Using PCA

The results of classifying ages using Principal Component Analysis technique are shown in Tables 5.21 to 5.23.

Table 5.21: Female, Male and Female+Male Second Step Age Classification Rates (%) with PCA on FGNET dataset

Gender	Classification 1	Classification 2
Female	77.55	61.84
Male	81.30	72.41
Female + Male	81.46	64.67

Table 5.22: Female, Male and Female+Male Second Step Age Classification Rates (%) with PCA on MORPH dataset

Gender	Classification 1	Classification 2
Female	58.82	70.00
Male	50.00	94.44
Female + Male	52.85	83.78

Table 5.23: Female, Male and Female+Male Second Step Age Classification Rates (%) with PCA on FGNET+MORPH dataset

Gender	Classification 1	Classification 2
Female	71.21	58.51
Male	65.73	73.40
Female + Male	72.72	64.00

5.3.4 Experiments Using ssLDA

Subspace LDA is implemented using maximum number of non-zero eigenvectors (no of classes -1). The second classification accuracies for age classification using ssLDA method are shown in Table 5.24. The following notations are used in the tables:

1: represents the first step classification performance,

2: represents the second step classification performance.

Table 5.24: Female and Male Second Step Age Classification Rates (%) with ssLDA on FGNET MORPH and FGNET+MORPH dataset

Gender	FGNET		MORPH		FGNET +MORPH	
	1	2	1	2	1	2
Female	74.48	63.01	79.72	48.83	64.70	40.90
Male	88.78	60.00	74.12	56.60	55.55	65

For the comparison of PCA and ssLDA as holistic approaches it can be concluded that the result of the second classification rate with PCA and ssLDA on FGNET dataset is better than MORPH and combined FGNET+ MORPH. The best result is

obtained with FGNET on male facial images due to the maximum rate in the fist and second step classification which is 81% and 72% respectively.

In general, the experiments on the second step classification demonstrate that LBP and PCA approaches achieve the better results on FGNET dataset in male facial images. It is clearly shown that second classification achieves the best classification rates when the rate of first step classification is high.

5.4 Ratio Analysis

Ratio analysis is applied on facial images in which primary features are located and labeled in order to separate babies from adults.

5.4.1 Age classification Experiments using two ratios

Ratio analysis is applied on 528 images of FGNET dataset, which includes 39 babies from 0 to 2 years old. Table 5.25 demonstrates the baby classification rate in FGNET dataset with different conditions.

Ratio1 values are obtained using

$$R_{em} = \frac{D_{em}}{D_{ee}}$$

and Ratio2 values are obtained using

$$R_{enm} = \frac{D_{en}}{D_{nm}}$$

Table 5.25: Baby Recognition Rates (%) with two Ratio analysis on FGNET dataset

Condition	Rate	Condition	Rate
Ratio1< 0.80	53.84	Average of Ratios < 1.52	53.84
Ratio1< 0.81	71.79	Average of Ratios < 1.56	87.17
Ratio1 < 0.82	100	Average of Ratios < 1.58	100
Ratio 2 < 1.31	69.23	Ratio1< 0.86 and ratio2 < 1.50	71.79
Ratio 2 < 1.34	76.92	Ratio1< 0.86 and ratio2 < 1.60	89.74
Ratio 2 < 1.35	79.48	Ratio1< 0.86 and ratio2 < 1.65	100
Ratio 2 < 1.36	87.17	Ratio1< 0.90 and ratio2 < 1.45	87.17
Ratio 2 < 1.37	97.43	Ratio1< 0.90 and ratio2 < 1.48	94.87

The values of Ratio1 and Ratio2 are closed to each other therefore the small change in the condition can change the accuracy of recognizing the babies. Using the ratio values can be reliable when all the images are frontal and the primary features are located carefully on the same line of coordinates. Using the ratio analysis cannot be an appropriate system alone because the differentiation is difficult.

Some values of Ratio 1 and Ratio 2 are shown in Table 5.26 and Table 5.27.

Table 5.26: Ratio1 and Ratio2 values of some FGNET images

Name	Age	Ratio1	Ratio2	AVG	Name	Age	Ratio1	Ratio2	AVG
019a00	0	0.78	1.21	1.00	072a27	27	0.90	2.26	1.58
023a00	0	0.83	1.28	1.05	001a28	28	1.03	2.20	1.61
015a01	1	0.81	1.78	1.30	061a29	29	0.90	1.90	1.40
073a01	1	0.89	1.95	1.42	072a29	29	0.95	2.25	1.60
011a02	2	0.84	1.30	1.07	005a30	30	1.04	1.98	1.51
026a02	2	0.90	2.30	1.60	029a31	31	0.98	1.52	1.25
002a03	3	0.87	1.35	1.11	061a32	32	0.89	1.54	1.22
046a04	4	0.89	1.94	1.42	067a33	33	0.87	2.11	1.49
011a05	5	0.89	1.57	1.23	012a34	34	0.99	2.09	1.54
008a06	6	0.78	1.72	1.25	062a35	35	0.95	1.39	1.17
081a07	7	0.89	1.79	1.34	006a36	36	0.98	1.36	1.17
001a08	8	0.91	2.24	1.57	028a37	37	0.94	1.52	1.23
060a08	8	0.88	1.69	1.28	002a38	38	0.95	1.41	1.18
035a09	9	1.01	1.56	1.29	021a39	39	1.11	1.83	1.47
037a09	9	0.84	1.37	1.11	011a40	40	0.94	1.59	1.27
056a10	10	0.94	1.63	1.29	072a41	41	0.97	2.73	1.85
081a10	10	0.89	2.37	1.63	017a42	42	1.00	1.89	1.44
075a11	11	0.90	1.97	1.43	045a43	43	1.04	1.74	1.39

Table 5.26 (continued)

Name	Age	Ratio1	Ratio2	AVG	Name	Age	Ratio1	Ratio2	AVG
031a12	12	1.01	1.98	1.49	071a44	44	0.91	1.48	1.19
036a13	13	0.94	1.93	1.44	007a45	45	0.96	1.62	1.29
050a14	14	0.98	1.89	1.43	048a46	46	0.97	1.67	1.32
056a15	15	0.85	2.11	1.48	004a48	48	0.92	2.56	1.74
082a16	16	1.03	1.97	1.50	048a49	49	0.92	1.71	1.31
076a17	17	0.88	2.09	1.48	048a50	50	0.92	1.62	1.27
001a18	18	0.95	2.73	1.84	004a51	51	0.97	2.13	1.55
005a18	18	1.01	2.08	1.54	039a52	52	0.97	1.71	1.34
061a19	19	0.92	1.64	1.28	048a54	54	1.00	1.84	1.42
002a20	20	0.99	2.26	1.62	047a55	55	0.93	1.73	1.33
082a21	21	0.94	1.52	1.23	003a58	58	1.04	1.89	1.47
007a22	22	0.99	1.50	1.25	003a60	60	1.01	2.13	1.57
057a23	23	1.00	1.97	1.48	005a61	61	0.94	1.79	1.36
071a23	23	0.94	1.66	1.30	006a61	61	1.01	1.29	1.15
005a24	24	1.07	2.16	1.62	004a62	62	1.00	1.74	1.37
061a25	25	0.88	1.64	1.26	004a63	63	0.95	3.29	2.12
002a26	26	0.99	1.74	1.36	006a67	67	1.00	1.38	1.19
048a27	27	0.98	1.66	1.32	006a69	69	1.04	1.29	1.16

Table 5.27: Ratio values of MORPH images

Name	Age	Ratio 1	Ratio 2	AVG
24928_1M28	28	0.82	1.40	1.11
30238_1M29	29	0.83	1.25	1.04
29201_0M30	30	0.94	1.26	1.10
42603_2M31	31	0.94	1.30	1.12
24928_2M32	32	0.92	1.43	1.17
42585_1M33	33	1.01	1.24	1.13
29201_1M36	36	0.98	1.08	1.03
30238_2M37	37	0.85	1.61	1.23
28926_2M38	38	0.98	1.33	1.15
30148_0M39	39	0.95	1.24	1.09
27534_3M42	42	0.91	1.53	1.22
28234_2M43	43	0.85	1.18	1.01
32752_1M45	45	1.06	0.66	0.86
24940_1M46	46	1.21	1.53	1.37
26845_1M47	47	0.89	1.26	1.07
32620_1M48	48	0.89	2.16	1.53
33027_1M50	50	0.95	1.18	1.06
32659_0M53	53	0.98	1.53	1.25
22008_2M55	55	1.15	1.19	1.17
9974_1M58	58	0.93	1.61	1.27
32659_1M61	61	0.92	1.76	1.34
27880_2M68	68	1.45	1.44	1.44

The values of Ratio1 and Ratio2 show that the value of Ratio1 and Ratio2 in babies is less than the values of Ratio1 in adults. It is not always true because all of the images are not frontal and the primary features are not in the same line of coordinates. Therefore, using ratio analysis algorithm may be not a reliable algorithm in all cases discussed above and it highly depends on facial images' poses.

Chapter 6

CONCLUSION

In this thesis, we have presented a performance analysis of subpattern-based LBP and subpattern-based mPCA approaches with holistic PCA and holistic ssLDA approaches for the solution of age classification problem. The experiments performed using three different datasets obtained from FG-NET and MORPH aging databases demonstrate the efficiency of LBP method over the other methods on both female and male facial images in first and second step classification. In the case of female age classification, LBP achieves better accuracies compared to mPCA, PCA and ssLDA performance on FG-NET and MORPH datasets. Age classification on male images demonstrates the superiority of LBP method on all datasets of FG-NET and MORPH. In general, it can be stated that LBP achieves better results for age classification on both female and male facial images for different datasets of FGNET and MORPH databases.

Future work on age classification can be focused on the following investigations:

- From a practical point of view, age classification methods should focus on the contributions of shape-based features and texture-based features in age classification from facial images.
- As a texture-based features algorithm, Weighted Local Binary Patterns (WLBP) can be used to investigate which regions are more important in aging process.

- Moreover, Support Vector Machines (SVM) in most of the classification algorithms have achieved the best accuracy in linear and nonlinear classification, therefore SVM can be applied for age classification to examine the accuracy rate in smaller age intervals.

REFERENCES

[1] A. Lanitis, C. Draganova, and C. Christodoulou. Comparing different classifiers for automatic age estimation. IEEE Transactions on Systems, Man, and Cybernetics, 34(1):621–628, 2004.

[2] Y. H. Kwon and N. da Vitoria Lobo, 'Age Classification from Facial Images', Computer Vision and Image Understanding Journal 74(1), pp. 1–21, 1999.

[3] http://www.scholarpedia.org/article/Facial_Age_Estimation

[4] Xin Geng, Zhi-Hua Zhou, and Kate Smith-Miles. Automatic age estimation based on facial aging patterns. IEEE Transactions on Pattern Analysis and Machine Intelligence, 29(12):2234–2240, 2007.

[5] Z. Yang and H. Ai. Demographic classification with local binary patterns. In Proc. of International Conference on Biometrics, pages 464–473, 2007.

[6] Y. Fu and T.S. Huang, 'Human Age Estimation with Regression on Discriminative Aging Manifold', IEEE Transactions on Multimedia, 10(4), pp 578-584, 2008

[7] M. G. Rhodes, 'Age Estimation of Faces: A Review'(2009), Appl. Cognitive Psychology. 23, pp 1–12.

[8] Ramanathan, N., Chellappa, R., Biswas, S. , “Age progression in Human Faces: A Survey”, Accepted for publication in Journal of Visual Languages and Computing (Special Issue on Advances in Multimodal Biometric Systems), 2009.

[9] L. S. Mark, J. T. Todd, and R. E. Shaw, “Perception of growth : A geometric analysis of how different styles of change are distinguished,” Journal of Experimental Psychology : Human Perception and Performance, vol. 7, pp. 855–868, 1981.

[10] N. Ramanathan, R. Chellappa, S. Biswas, Computational Methods for Modeling Facial Aging: A Survey, Journal of Visual Languages and Computing, 2009.

[11] J. Huang, B. Heisele and V. Blanz, Component-based Face Recognition with 3D Morphable Models, *AVBPA*, 2003.

[12] P. Pujol, D. Macho, C. Nadeu, “On Real-Time Mean-and-Variance Normalization of Speech Recognition Features”. IEEE International Conference on Acoustics, Speech and Signal Processing, 2006. ICASSP 2006 Proceedings. Volume 1, I–I, 14-19 May 2006.

[13] Z. Gengtao, Z. Yongzhao, Z. Jianming, “Facial Expression Recognition Based on Selective Feature Extraction”. Sixth International Conference on Intelligent Systems Design and Applications, 2006. ISDA '06. Volume 2, 412-417, Oct. 2006.

[14] T. Ojala, M. Pietika¨inen, and D. Harwood, “A Comparative Study of Texture Measures with Classification Based on Feature Distributions,” Pattern Recognition, vol. 29, no. 1, pp. 51-59, 1996.

[15] T.Ahonen, M.Pietikainen, “Face Description with Local Binary Patterns: Application to Face Recognition,” IEEE Trans. Pattern Analysis and Machine Intelligence, vol. 28, no. 12, December 2006.

[16] T. Ojala, M. Pietikainen, and T. Ma¨enpa¨a¨, “Multiresolution Gray-Scale and Rotation Invariant Texture Classification with Local Binary Patterns,” IEEE Trans. Pattern Analysis and Machine Intelligence, vol. 24, no. 7, pp. 971-987, July 2002.

[17] P.N. Belhumeur, J.P. Hespanha, D.J. Kriegman, Eigenfaces vs. Fisherfaces: Recognition Using Class Specific Linear Projection, IEEE Trans. Pattern Analysis and Machine Intelligence, 19(7), 1997, 711-720.

[18] X. Wang, and X. Tang, Random Sampling for Subspace Face Recognition, Interntional Journal of Computer Vision, 70(1), 2006, 91-104.

[19] Vytautas Perlibakas, “Distance measures for PCA-based face recognition”. Pattern Recognition Letters, Volume 25, Issue 6, 711-724, 19 April 2004.

[20] R. Gottumukkal and V.K. Asari, An improved face recognition technique based on modular PCA approach, Pattern Recogn. Lett. 25 (2004) (4), pp. 429–436

[21] S. Chen, Y. Zhu, Rapid and Brief Communication Subpattern-based principal component analysis. 3 September 2003, Pattern Recognition Society, Volume 37, Issue 5, May 2004, Pages 1081-1083

[22] J. Huang, B. Heisele and V. Blanz, Component-based Face Recognition with 3D Morphable Models, *AVBPA*, 2003.

[23] M. Turk and A. Pentland, Eigenfaces for Recognition, Journal of Cognitive Neuroscience, 3(1), 1991, 71-96.

[24] P.N. Belhumeur, J.P. Hespanha, D.J. Kriegman, "Eigenfaces vs. Fisherfaces: Recognition Using Class Specific Linear Projection", IEEE Trans. Pattern Analysis and Machine Intelligence, 19(7), 1997, 711-720.

[25] F. Song, H. Liu, D. Zhang, J. Yang, A Highly Scalable Incremental Facial Feature Extraction Method, Neurocomputing, 71, 2008, 1883-1888.

[26] L. S. Mark, J. B. Pittenger, H. Hines, C. Carello, R. E. Shaw, and J. T. Todd, "Wrinkling and head shape as coordinated sources of age level information," Journal of Perception and Psychophysics, vol. 27(2), pp. 117–124, 1980.

[27] W. B. Horng, C. P. Lee and C. W. Chen "Classification of Age Groups Based on Facial Features", *Tamkang Journal of Science and Engineering*, Vol. 4, No. 3, pp. 183-192, 2001.

[28] http://www.isbe.man.ac.uk/~bim/software/am_tools_doc/index.html

[29] The FG-NET Aging Database:
http://sting.cycollege.ac.cy/~alanitis/fgnetaging/index.htm

[30] Ricanek, K., Tesafaye, T., "MORPH: A Longitudinal Image Database of Normal Adult Age-Progression ", 7th International Conference on Automatic Face and Gesture Recognition, Southampton, UK, pp 341-345 (2006).

[31] G. Guo, Y. Fu, C. R. Dyer, and T.S. Huang, 'Image-Based Human Age Estimation by Manifold Learning and Locally Adjusted Robust Regression', IEEE Transactions On Image Processing, 17(7), pp 1178-1188, 2008.

[32] Lanitis, A., "A survey of the effects of aging on biometric identity verification, "International Journal of Biometrics (IJBM), Vol. 2, No. 1, pp. 34 – 52 (xxxx).

[33] TorchVision C++ Program, http://www.torch3vision.idiap.ch